

Signaling through the Leukocyte Integrin LFA-1 in T Cells Induces a Transient Activation of Rac-1 That Is Regulated by Vav and PI3K/Akt-1*

Received for publication, January 28, 2004

Published, JBC Papers in Press, February 11, 2004, DOI 10.1074/jbc.M400905200

Lorena Sánchez-Martín^{‡§}, Noelia Sánchez-Sánchez^{‡§}, M. Dolores Gutiérrez-López[‡], Ana I. Rojo[¶], Miguel Vicente-Manzanares[¶], María José Pérez-Alvarez[‡], Paloma Sánchez-Mateos^{**}, Xosé R. Bustelo^{‡‡}, Antonio Cuadrado[¶], Francisco Sánchez-Madrid[¶], José Luis Rodríguez-Fernández^{‡§§}, and Carlos Cabañas^{‡||§§¶¶}

From the [‡]Instituto de Farmacología y Toxicología (CSIC-UCM), Facultad de Medicina UCM, Madrid 28040, [¶]Departamento de Bioquímica (CSIC-UAM), Facultad de Medicina, Universidad Autónoma de Madrid, Madrid 28029, ^{**}Sección de Inmuno-Oncología, Hospital Gregorio Marañón, Madrid 28007, ^{||}Servicio de Inmunología, Hospital de la Princesa, Madrid 28006, and ^{‡‡}Centro de Investigación del Cáncer (CSIC-USAL), Universidad de Salamanca, Salamanca 37007, Spain

Integrin LFA-1 is a receptor that is able to transmit multiple intracellular signals in leukocytes. Herein we show that LFA-1 induces a potent and transient increase in the activity of the small GTPase Rac-1 in T cells. Maximal Rac-1 activity peaked 10–15 min after LFA-1 stimulation and rapidly declined to basal levels at longer times. We have identified Vav, a guanine nucleotide exchange factor for Rac-1, and PI3K/Akt, as regulators of the activation and inactivation phases of the activity of Rac-1, respectively, in the context of LFA-1 signaling based on the following experimental evidence: (i) LFA-1 induced activation of Vav and PI3K/Akt with kinetics consistent with a regulatory role for these molecules on Rac-1, (ii) overexpression of a constitutively active Vav mutant induces activation of Rac-1 independently of LFA-1 stimulation whereas overexpression of a dominant-negative Vav mutant blocks LFA-1-mediated Rac activation, (iii) pharmacological inhibition of PI3K/Akt prevented the fall in the activity of Rac-1 after its initial activation but had no effect on Vav activity, and (iv) overexpression of a dominant-negative or a constitutively active Akt-1 induced or inhibited, respectively, Rac-1 activity. Finally, we show that T cells with a sustained Rac activity have impaired capacity to elongate onto ICAM-1. These results demonstrate that down-regulation of the activity of this GTPase is a requirement for the regulation of T cell morphology and motility and highlight the importance of temporal regulation of the signaling triggered from this integrin.

T lymphocytes are primarily circulating cells in the vascular system until they sense signals that trigger their adhesion to endothelial cells and their migration across the endothelial monolayer into the subendothelial tissue. Acquisition of a polarized phenotype by T lymphocytes is an essential feature that is required for crucial functions performed by these cells, including extravasation, oriented migration toward inflammatory sites, and interaction with antigen presenting cells during antigen recognition (1–3).

The integrin LFA-1 (lymphocyte function-associated antigen-1, also known as CD11a/CD18 or $\alpha_L\beta_2$) is a member of the leukocyte (β_2) subfamily of integrins that is expressed on the cell surface of all leukocytes (4, 5). This molecule mediates important adhesive phenomena through interactions with its ligands intercellular adhesion molecules (ICAM-1,¹ -2, or -3). Resting T lymphocytes express an inactive form of the integrin LFA-1 with low affinity/avidity for its ligands. However, leukocyte activation through different cell surface receptors, including the T cell receptor-CD3 complex and receptors for cytokines and chemokines, results in activation of LFA-1 molecules (6–8). Activation of LFA-1 molecules can also be induced from outside the cells by different protocols, including (i) induction of integrin clustering following cross-linking with a secondary antibody, (ii) altering the extracellular divalent cation conditions, *i.e.* by addition of micromolar concentrations of Mn^{2+} (9), or (iii) addition of specific activating or stimulatory mAbs (such as the CD18-specific mAb KIM-127 (10, 11) that, upon binding to the α or the β subunits of LFA-1, alter the conformation of the integrin to a state of increased affinity for its ligands.

Integrins are currently recognized to work not merely as adhesion molecules but as cell surface receptors capable of efficiently transducing a variety of signals to the cell interior. For integrin LFA-1 in particular, the intracellular signals that are generated in T cells following ligand engagement of this receptor have not been fully characterized. It has been described that LFA-1 signaling includes phosphorylation of phos-

* This work was supported in part by Grants CICYT SAF 2001–2807 from Ministerio de Ciencia y Tecnología and FIS-01/1367 from Ministerio de Sanidad y Consumo (to C. C.), a fellowship from Comunidad de Madrid (to L. S.-M.), a Formación de Profesorado Universitario predoctoral fellowship from Ministerio de Educación, Cultura y Deporte (to N. S.-S.), and a postdoctoral fellowship from Ministerio de Educación, Cultura y Deporte (to M. D. G.-L.). The costs of publication of this article were defrayed in part by the payment of page charges. This article must therefore be hereby marked “advertisement” in accordance with 18 U.S.C. Section 1734 solely to indicate this fact.

§ Contributed equally to this work.

§§ Senior author. Contributed equally to this work.

¶¶ To whom all correspondence should be addressed: Instituto de Farmacología y Toxicología (CSIC-UCM), Facultad de Medicina UCM, Pabellón III, Madrid 28040, Spain. Tel.: 34-91-3941444; Fax: 34-91-3941470; E-mail: cacabagu@med.ucm.es.

¹ The abbreviations used are: ICAM-1, intercellular adhesion molecule; mAb, monoclonal antibody; PI3K, phosphoinositide 3-kinase; GEF, guanine nucleotide exchange factor; BSA, bovine serum albumin; EGFP, enhanced green fluorescent protein; DN, dominant-negative; CA, constitutively active; SH, Src homology; PBS, phosphate-buffered saline; PMSF, phenylmethylsulfonyl fluoride; PAK, p-21 activated kinase.

pholipase C γ 1, phospholipid hydrolysis, activation of different isoenzymes of protein kinase C, mobilization of intracellular Ca²⁺, and activation of tyrosine kinases (12–18). We have reported recently that activation of integrin LFA-1 on T lymphocytes and subsequent cell adhesion onto immobilized ligand ICAM-1 leads to a T cell phenotype characterized by strong adhesion, acquisition of an elongated morphology, cessation of cell motility, and activation of the intracellular tyrosine kinase PYK-2 (17–19). These events become apparent 30–40 min after activation of LFA-1 and adhesion of cells and were completely dependent on the reorganization of actin cytoskeleton, because they were completely blocked by cytochalasin D (17).

Phosphoinositide 3-kinases (PI3Ks) are a family of intracellular signal transducing enzymes that share the capacity to phosphorylate phosphatidylinositol lipids at the D-3 position of the inositol ring. Three classes of PI3Ks have been defined based on their structure and subunit composition, substrate specificity, and regulatory mechanisms. Class I PI3Ks are the best characterized in leukocytes. The lipid products of class I PI3Ks are involved in the coordination of a set of events leading to cell growth, cell cycle entry, cell migration, and cell survival, through the targeting of numerous cytosolic proteins that contain domains that specifically bind to D-3 phosphorylated phosphoinositides. The fungal metabolite wortmannin and the pharmacological compound LY294002 are two potent inhibitors of class I PI3Ks that have been used extensively to study the physiological role of class I PI3Ks in various cellular responses. Through the use of these inhibitors, class I PI3Ks have been shown to play an important role in the control of chemotactic peptide- and chemokine-induced polarization and cytoskeletal organization in leukocytes (20, 21). The serine-threonine kinase Akt-1 is a major target of PI3K that plays a role in protecting many cell types from apoptosis and in promoting cell survival (22, 23). Recently, the PI3K/Akt-1 pathway has also been involved in the control of neutrophil chemotaxis (24). Akt-1 is activated by phosphorylation by the kinase PDK-1, following binding through its pleckstrin homology domain to the PI3K lipid products on the plasma membrane.

Members of the Rho subfamily of small GTPases, including Rho, Rac, and Cdc42, play crucial roles in the regulation of cytoskeletal organization in many cell types, including leukocytes (25–29). The Rho family member Rac-1 has been shown to be essential for cytoskeletal changes and spreading, polarization and chemotaxis of different leukocyte populations on fibronectin and other ligands for β 1 integrins (30–33). These proteins cycle between a GDP-bound state (inactive) and a GTP-bound (active) state that is able to interact and activate their downstream signaling effectors. The intrinsic GTPase activity of Rho family GTPases is potentiated by GTPase-activating proteins that therefore favor the inactive state (GDP-bound) of these GTPases whereas guanine nucleotide exchange factors (GEFs) induce the release of GDP and binding of new GTP. Vav is 95-kDa multidomain protein that works as a key GEF for Rac GTPases in hematopoietic cells. In T lymphocytes Vav is involved in the T cell receptor signaling that leads to activation of Rac-1 and cytoskeletal rearrangements (34). Vav guanine exchange activity is primarily regulated through phosphorylation by different intracellular tyrosine kinases of the Src and Syk families although binding of Vav through its pleckstrin homology domain to phosphoinositide products of PI3K may represent an additional level of regulation of the activity of this GEF (35–37). In this paper, we show that following LFA-1 activation and ligand engagement in T lymphocytes the Rho family member Rac-1 is transiently activated. Furthermore, we demonstrate that LFA-1 induces activation of Vav and PI3K/Akt, which in turn regulate the activation and

inactivation of Rac-1, respectively. By transfecting T cells with constitutively active mutant forms of Vav and Rac-1 and through pharmacological inhibition of PI3K/Akt-1 we show that the inactivation of Rac-1 is necessary for the processes of T cell polarization and motility mediated by LFA-1.

MATERIALS AND METHODS

Cell Culture—Human T lymphoblasts were prepared from peripheral blood mononuclear cells by treatment with 10 μ g/ml phytohemagglutinin (Amersham Biosciences) for 48 h as described previously (9). Cells were washed and cultured in RPMI 1640 (BioWhittaker) containing 10% fetal calf serum (Harlan Sera-Lab.) 50 units/ml penicillin, 50 mg/ml streptomycin (P/E; BioWhittaker), 2 mM L-glutamine (L-Gln; BioWhittaker), and 50 units/ml interleukin-2 (Eurocetus). T lymphoblasts cultured by 10–12 days were typically used in all experiments. The human T cell line HSB-2 was cultured in RPMI 1640, 10% fetal calf serum, 50 units/ml penicillin/2 mM L-glutamine, and 50 mg/ml streptomycin.

Antibodies and Reagents—ICAM-1-Fc chimeric protein consisting of the five domains of ICAM-1 fused to the Fc fragment of human IgG1 was prepared as described (38). The anti-CD18 mAb Lia3/2.1 (39) was purified from mouse ascites by protein A affinity chromatography. The monoclonal antibody KIM-127 was obtained from Dr. Martin Robinson (Celltech Group, Berkshire, United Kingdom) (40). Anti-p85 PI3K polyclonal antibody was from Upstate Biotechnology (Lake Placid, NY). The anti-phospho-Akt-Ser⁴⁷³ and anti-Akt-1 polyclonal antibodies were from Pharmingen. The monoclonal antibodies anti-Rac-1, anti-PY20, and polyclonal anti-Vav1 were from Transduction Laboratories. Anti-PYK-2 (C-19) polyclonal antibody was from Santa Cruz. The polyclonal anti-phospho-Tyr¹⁷⁴-Vav antibody, which specifically detects active Vav, has been described previously (41). The antibody that recognizes the consensus sequence RLRPLpS/pT that is phosphorylated by Akt-1 was purchased from Cell Signaling (Beverly, MA). The polyclonal anti-phospho-Ser antibody was from Zymed Laboratories Inc. (San Francisco, CA). The monoclonal anti-AU5 and anti-AU1 antibodies were from Covance (Berkeley, CA). [γ -³²P]ATP (6000 Ci/mmol) were from American Radiolabeled Chemicals. BSA, poly-lysine, LY294002, L- α -phosphatidylinositol, protein A-agarose, protein G-agarose, glutathione-agarose, polyclonal anti-mouse-IgG, and secondary peroxidase-conjugated antibodies were from Sigma. Wortmannin, genistein, and isopropyl-1-thio- β -D-galactopyranoside were from Calbiochem. Oxylated silica gel plates were from Merck. The enhanced chemiluminescent solution (ECL) was from Amersham Biosciences.

Expression Constructs and Transient Transfection Assays—The pEGFP-C1 expression vector obtained from Clontech (Palo Alto, CA), the dominant-negative Rac (DN-Rac) pEGFP-C1-N17Rac expression plasmid, and the constitutively active Rac cDNA (CA-Rac) pEGFP-C1-V12Rac expression plasmid have been described previously (31). The pDNA3-AU1BAD and pCEFL-AU5Rac-1, termed Rac-1-AU5 and BAD-AU1, respectively, were described previously (42, 43). Kinase-dead EGFP-Akt-1 (K179M), which acts as a dominant-negative (DN-Akt-1), and myr-EGFPAkt-1, which acts as a constitutively active mutant (CA-Akt-1) of Akt-1, respectively, have been described elsewhere (44, 45). The CA-Vav construct pEGFP-C2-Vav-(Δ 1–186) and the DN-Vav construct that only contains the SH3-SH2-SH3 domains of Vav (pEGFP-C2-SH3-SH2-SH3-Vav) have been described previously (37). For transient transfection experiments, HSB-2 cells (3.5×10^7) were washed twice with cold RPMI and resuspended in 500 μ l of cold Opti-MEM (Invitrogen) before being placed in a 0.4-cm electroporation cuvette (BTX Instruments, Holliston, MA). DNA (15 μ g) was added, and transfections were conducted at 310V 2 pulses for 10 ms using a ECM830 BTX electroporation system. After the electroporation bursts, the cells were transferred to plastic dishes and cultured in RPMI 1640 containing 10% fetal calf serum and 2 mM L-glutamine. Transfection efficiencies were estimated by flow cytometry 16–24 h after electroporation.

Cell Attachment and Morphological Analysis of T Cells—Induction of T cell adhesion to either ICAM-1 or poly-L-lysine-coated dishes was performed as described elsewhere (17). Briefly, 96-well flat-bottom plates and 35- and 90-mm dishes were pre-coated overnight at 4 $^{\circ}$ C with 5 μ g/ml ICAM-1-Fc in PBS, blocked with 1% BSA in PBS for 1 h at room temperature, and then washed twice with RPMI 1640. In control integrin-independent adhesion experiments, wells or dishes were pre-coated overnight at 4 $^{\circ}$ C with 20 μ g/ml poly-L-lysine in PBS. T cells were washed twice with RPMI 1640 and starved in RPMI 1640 without serum for 90 min. In some cases cells were pre-treated for 30 min at 37 $^{\circ}$ C with the PI3K inhibitors (100 μ M LY294002 or 100 nM wortman-

nin). After this pre-incubation, cells were plated on the dishes and stimulated or not by the addition of 200 μM Mn^{2+} or 10 $\mu\text{g}/\text{ml}$ KIM-127 mAb to activate LFA-1. Cells were then incubated at 37 °C for different periods of time prior to lysis and further analysis of Rac-1, Vav, PI3K, Akt-1, or PYK-2. For morphological studies, T cells were allowed to adhere for 90 min and then unbound cells were removed by three washes with PBS. Attached cells were fixed in 3% formaldehyde in PBS for 10 min at room temperature, permeabilized in 2% methanol in PBS for 5 min at room temperature, and stained with 0.5% crystal violet in 20% methanol. The morphological changes were analyzed by microscopy.

LFA-1 Cross-linking Activation—T cells (5–20 $\times 10^6$ cells for each condition) were washed twice and starved in RPMI 1640 with 20 mM Hepes (RPMI-Hepes) for 90 min. Cells were then pre-treated or not for 30 min at 37 °C with the PI3K inhibitors (100 μM LY294002 or 100 nM wortmannin). After this period, cells were treated with the anti-LFA-1 mAb Lia3/2.1 (10 $\mu\text{g}/\text{ml}$) and incubated with gentle rotation for an additional period of 50 min at 4 °C. Unbound antibody was removed by subjecting the cells to three washes in 20 mM Hepes/RPMI medium. LFA-1 was cross-linked by adding polyclonal anti-mouse-IgG (25 $\mu\text{g}/\text{ml}$) in 20 mM Hepes/RPMI medium. Finally, cells were washed once with cold 20 mM Hepes/RPMI medium and lysed in the appropriate buffer (see “Immunoprecipitation and Western Blotting”).

Immunoprecipitation and Western Blotting—For PI3K immunoprecipitation, cells were lysed in Buffer A (20 mM Tris, pH 7.4, 1% Triton X-100, 40 mM NaCl, 1 mM Na_3VO_4 , 1 mM PMSF, 10 $\mu\text{g}/\text{ml}$ leupeptin, 5 $\mu\text{g}/\text{ml}$ aprotinin, 10 $\mu\text{g}/\text{ml}$ pepstatin, 10% glycerol). To study Akt-1 phosphorylation cells were lysed in Buffer B (20 mM Tris-HCl, pH 7.5, 1% Nonidet P-40, 137 mM NaCl, 20 mM NaF, 1 mM NaPP_i, 1 mM Na_3VO_4 , 10 $\mu\text{g}/\text{ml}$ leupeptin, 5 $\mu\text{g}/\text{ml}$ aprotinin, 10 $\mu\text{g}/\text{ml}$ pepstatin, 1 mM PMSF, 10% glycerol). For Vav analysis cells were lysed in Buffer C (25 mM Tris-HCl, pH 7.8, 1% Triton X-100, 1 mM EDTA, 20 mM NaF, 1 mM Na_3VO_4 , 1 mM NaPP_i, 10 $\mu\text{g}/\text{ml}$ leupeptin, 5 $\mu\text{g}/\text{ml}$ aprotinin, 10 $\mu\text{g}/\text{ml}$ pepstatin, 1 mM PMSF, 10% glycerol). Cells used to study PYK-2 were lysed in Buffer D (10 mM Tris, pH 7.6, 5 mM EDTA, 50 mM NaCl, 30 mM NaPP_i, 50 mM NaF, 2.1 mM Na_3VO_4 , 1% Triton X-100, 50 $\mu\text{g}/\text{ml}$ leupeptin, 50 $\mu\text{g}/\text{ml}$ aprotinin, 5 $\mu\text{g}/\text{ml}$ pepstatin, 1 mM PMSF). In Rac phosphorylation studies, cells were lysed in Buffer E (50 mM Tris-HCl, pH 7.4, 1% Nonidet P-40, 137 mM NaCl, 10% glycerol, 5 mM MgCl_2 , 20 mM NaF, 1 mM NaPP_i, 1 mM Na_3VO_4 , 10 $\mu\text{g}/\text{ml}$ leupeptin, 5 $\mu\text{g}/\text{ml}$ aprotinin, 10 $\mu\text{g}/\text{ml}$ pepstatin, 1 mM PMSF). All lysates were clarified by centrifugation at 14,000 rpm for 15 min, and the pellets were discarded. For PI3K, Vav, Rac phosphorylation, and PYK-2 assays, immune complexes from supernatants were precipitated overnight at 4 °C with protein A or protein G linked to agarose. Immunoprecipitates were washed three times with the specific lysis buffer and either used for PYK2/PI3K *in vitro* kinase reactions or extracted in 2 \times SDS-PAGE sample buffer (200 mM Tris-HCl, pH 6.8, 0.1 mM Na_3VO_4 , 1 mM EDTA, 6% SDS, 4% 2-mercaptoethanol, and 10% glycerol) and boiled for 5 min for one-dimensional SDS-PAGE. To analyze Akt activation, clarified lysates were extracted in 5 \times SDS-PAGE sample buffer whereas to study Rac phosphorylation Rac-AU5 from clarified lysates was immunoprecipitated and then extracted in 2 \times SDS-PAGE sample buffer. After SDS-PAGE, proteins were transferred to nitrocellulose or polyvinylidene difluoride membranes. Membranes were blocked using 3% nonfat dried milk or 3% BSA in PBS and incubated with the appropriate antibodies. Immunoreactive bands were visualized using enhanced chemiluminescence reagents.

PI3K *In Vitro* Kinase Reactions—Reactions were performed as described (46). Briefly, immunoprecipitates were washed and pelleted three times in Lysis Buffer A (see “Immunoprecipitation and Western Blotting”) and twice with kinase buffer (20 mM Tris-HCl, 7.5 mM NaCl, 20 mM Hepes, 10 mM MgCl_2 , 200 mM adenine). Pellets were dissolved in 50 μl of kinase buffer, and the reaction was started by adding 5 μCi of [γ -³²P]ATP and 20 μg of L- α -phosphatidylinositol. The mixture was incubated at room temperature for 15 min, and the reaction was stopped by adding 100 μl of chloroform. Lipids were extracted by adding 200 μl of chloroform:methanol:HCl (100:200:2, v/v). After centrifugation at 3,000 rpm at 4 °C, 50 μl of the lower organic phase was applied to an oxylated silica gel plate. Lipids were resolved by thin-layer chromatography using a solvent mixture of chloroform:methanol:water (75:20:5, v/v). Phosphatidylinositol 3-phosphate was detected by autoradiography.

PYK-2 *In Vitro* Kinase Reactions—Reactions were performed as described (17, 19). Briefly, immunoprecipitates were washed and pelleted three times in Lysis Buffer D and twice with kinase buffer (20 mM Hepes and 3 mM MnCl_2 , pH 7.35). Pellets were dissolved in 40 μl of kinase buffer, and the reactions were started by adding 10 μCi of [γ -³²P]ATP. Reactions were carried out at 30 °C for 15 min and then

stopped on ice by adding 10 mM EDTA. Pellets were washed in lysis buffer containing 10 mM EDTA, extracted for 5 min at 90 °C in 2 \times SDS-PAGE sample buffer, and analyzed by SDS-PAGE and autoradiography.

Rac-1 Pull-down Activity Assays—GST-PAK-CRIB fusion proteins were a kind gift from Dr. J. G. Collard (The Netherlands Cancer Institute, Amsterdam, The Netherlands). Rac activity assays were performed with slight modifications as described previously by Sander *et al.* (47). In brief, after induction of LFA-1 activation (by Mn^{2+} or KIM-127-induced adhesion to ICAM-1 or cross-linking) and/or transfection with relevant constructs, T cells were lysed in 500 μl of ice-cold Lysis Buffer E (50 mM Tris-HCl, pH 7.4, 1% Nonidet P-40, 137 mM NaCl, 10% glycerol, 5 mM MgCl_2 , 20 mM NaF, 1 mM NaPP_i, 1 mM Na_3VO_4 , 10 $\mu\text{g}/\text{ml}$ leupeptin, 5 $\mu\text{g}/\text{ml}$ aprotinin, 10 $\mu\text{g}/\text{ml}$ pepstatin, 1 mM PMSF). Lysates were cleared by centrifugation, and 15 μl of these samples were used for loading controls. Cleared lysates were incubated overnight at 4 °C with GST-PAK-CRIB coupled to glutathione-agarose beads to precipitate GTP-bound Rac-1. Precipitated complexes were washed three times in ice-cold Lysis Buffer E and boiled in sample buffer (100 mM Tris-HCl, pH 6.8, 0.05 mM sodium orthovanadate, 0.5 mM EDTA, 3% SDS, 2% 2-mercaptoethanol, and 5% glycerol). Proteins from total lysates and precipitates were fractionated by 15% SDS-PAGE, transferred to polyvinylidene difluoride membranes, and immunoblotted with anti-Rac-1 mAb.

Time-lapse Fluorescence Microscopy—HSB-2 T cells were transiently transfected with CA-Vav cDNA or CA-Rac cDNA (see “Expression Constructs and Transient Transfection Assays”) as described above and grown in complete RPMI 1640 medium for 16–24 h. Then, after removal of death cells by a Ficoll gradient, cells were starved for 90 min, resuspended in 1 ml of 20 mM Hepes-RPMI 1640 medium, and plated onto 35-mm dishes that had been coated previously with 2.5 $\mu\text{g}/\text{ml}$ ICAM-1-Fc overnight at 4 °C and saturated with 1% heat-denatured BSA for 2 h at room temperature. LFA-1 on T cells was activated with mAb KIM-127 (10 $\mu\text{g}/\text{ml}$) or with MnCl_2 (200 μM), and cells were recorded for a period of 90 min. Fluorescence and phase contrast images were acquired at 20-s intervals with a $\times 40$ objective on a Leica DM-IRE2 microscope equipped with digital camera and Q-fluoro time-lapse Leica Software.

RESULTS

LFA-1 Induces Transient Activation of the Small GTPase Rac-1—Because the Rho family member Rac-1 GTPase is a major regulator of the organization of the actin cytoskeleton in most cell types including T lymphocytes (31, 48), we decided to explore in more detail whether the activity levels of this small GTPase in T cells are altered following LFA-1 activation and ligand engagement. Pull-down assays using the fusion protein GST-PAK-CRIB, a Rac-1 binding domain of the PAK effector molecule that only binds the active GTP-bound-Rac-1, and glutathione-agarose were performed to detect changes in the activity of Rac-1 in T lymphoblasts at various time periods after induction of LFA-1 activation. Three different protocols to induce LFA-1 activation and signaling were used: (i) addition of 200 μM divalent cation Mn^{2+} to the extracellular medium and adhesion onto ligand ICAM-1 (Fig. 1A), (ii) use of the stimulatory anti-CD18 mAb KIM-127 and adhesion onto ICAM-1 (Fig. 1B), and (iii) induction of clustering of the LFA-1 molecules by cross-linking with the specific anti-CD18 mAb Lia3/2.1 (Fig. 1C). Interestingly, as shown in Fig. 1, a transient increase in the activity of Rac-1 is consistently observed following the induction of LFA-1 activation and signaling regardless of the method employed. Maximal levels of Rac-1 activation (almost 6-fold) were detected 10–15 min after LFA-1 activation and then declined to basal levels at longer times (30 min). Identical transient kinetics of Rac-1 activity was observed when the activation of integrin LFA-1 was induced on the HSB-2 T cell line (not shown), indicating that this phenomenon is not restricted to a particular T cell type.

LFA-1 Mediates Rac Activation through the GEF Vav—The transient nature of Rac-1 activation following LFA-1 stimulation suggests that distinct upstream signaling components might be responsible for the initial increase in Rac-1 activity

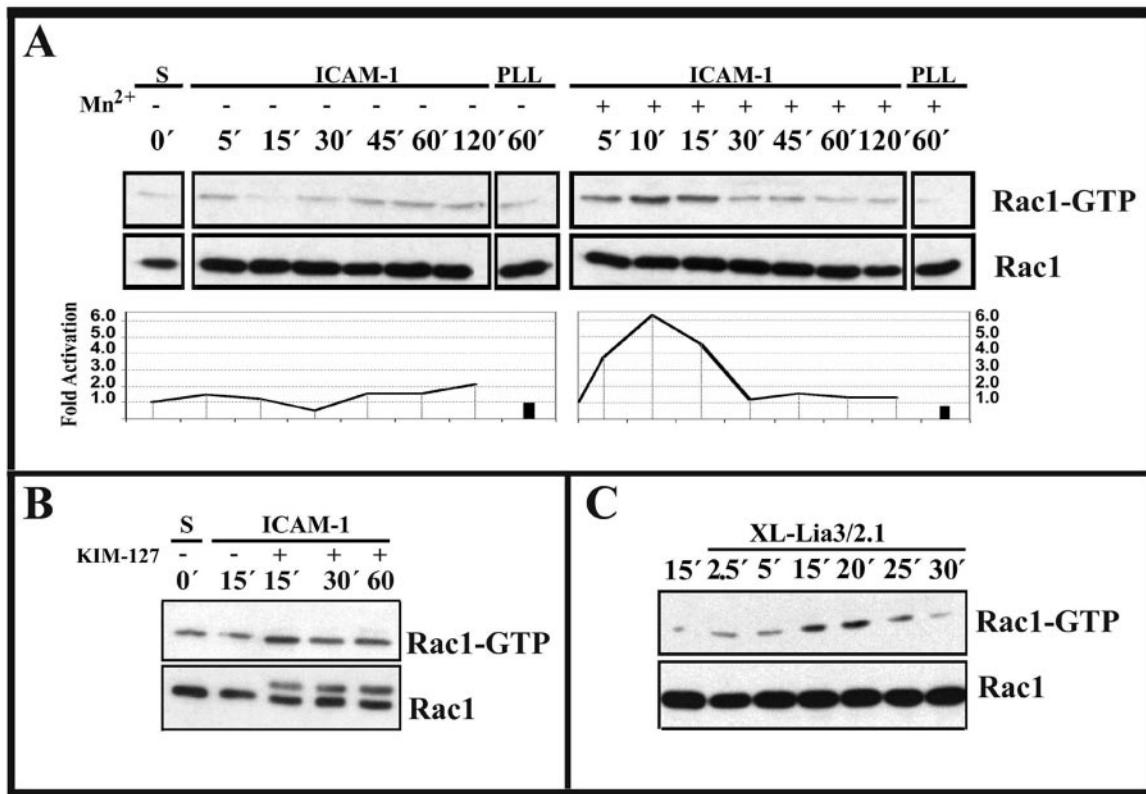


FIG. 1. LFA-1 induces transient activation of Rac-1 in T cells. Rac-1 activity was analyzed in T lymphoblasts. LFA-1 was activated for different time periods, cells were lysed, and Rac-1 activated fraction (*Rac-1-GTP*) was pulled down using GST-PAK-CRIB-agarose beads. Aliquots from lysates were also used to analyze the total levels of Rac-1 by Western blotting using an anti-Rac-1 mAb. Three different protocols were used to induce activation of LFA-1. **A**, T lymphocytes were allowed to adhere onto ICAM-1 or poly-L-lysine-coated dishes, and LFA-1 was stimulated (+) or not (–) with 200 μ M MnCl₂. -Fold activation of Rac-1 over basal levels was quantified, and the kinetics of activation is represented. **B**, LFA-1 was activated with the stimulatory anti-CD18-specific mAb KIM-127. Cells were then allowed to adhere onto ICAM-1-coated dishes for the times indicated before lysis and pull-down assays. The *upper band* that appears in some of the Rac-1 loading controls corresponds to the KIM-127 antibody light chain. **C**, LFA-1 was directly clustered by cross-linking (*XL-Lia3/2.1*) of the anti-CD18 mAb Lia3/2.1 with a secondary antibody.

(activation phase) and for the subsequent return to basal activity (inactivation phase) observed at longer times. Vav is a GEF that has been demonstrated to increase the activity of Rac-1 in several hematopoietic cell types (34). Moreover, tyrosine phosphorylation of Vav has been shown to mediate activation of p21Ras following β 2 integrin triggering in neutrophils (49). Thus, it was of interest to determine whether activation of Vav could account for the initial increase in Rac-1 activity following LFA-1 stimulation in T lymphocytes. For this purpose, cross-linking of the anti-LFA-1 mAb Lia3/2.1 was used to induce signaling from this integrin in HSB-2 T cells. Fig. 2A shows that Vav was rapidly and transiently phosphorylated following antibody-induced clustering of LFA-1 in HSB-2 T cells. The maximal phosphorylation of Vav was observed 2–5 min after ligation of the integrin, returning to basal levels at longer times. As tyrosine phosphorylation can result in both activation and down-modulation of the activity of Vav (41, 50), we have also analyzed more specifically the LFA-1-mediated activation of Vav by Western blot using a specific antibody that recognizes active Vav (phospho-Tyr¹⁷⁴) (41, 50). As shown in Fig. 2B, LFA-1 stimulation induces the activation of Vav at 2 min. Pretreatment of cells with the PI3K inhibitor LY294002 did not affect the activation of Vav. This rapid kinetics of Vav activation and subsequent return to basal activity was compatible with its function as a GEF responsible for the initial activation Rac-1. Further support for the role of Vav as a key GEF for Rac-1 in T lymphocytes was obtained by transiently transfecting HSB-2 cells with constitutively active and dominant-negative forms of Vav (CA-Vav and DN-Vav). Fig. 2C shows that in HSB2 cells transfected with CA-Vav the basal

levels of GTP-Rac-1 (in the absence of LFA-1 stimulation) were enhanced compared with cells transfected with control pEGFP plasmid. Interestingly DN-Vav reduced Rac-1 activity below basal levels, and LFA-1 cross-linking could not activate Rac. Altogether, these results suggest the important role of this GEF in the regulation of Rac-1 activity in T cells following LFA-1 engagement.

LFA-1 Induces Transient Activation of PI3K—Several reports have demonstrated a central role for PI3K in integrin-mediated cellular responses in a variety of cells, including different types of leukocytes (22). We decided to study whether PI3K was also implicated in the observed LFA-1-driven activation of Rac-1 in T cells. We first analyzed the changes in activity of this intracellular enzyme at different times after the induction of activation of LFA-1. For this purpose, T lymphoblasts were plated on dishes coated with ligand ICAM-1 and treated for different time periods with Mn²⁺ to induce the activation of LFA-1. After these treatments T cells were lysed, PI3K was immunoprecipitated, and the resulting immunocomplexes incubated with [γ -³²P]ATP (see “Materials and Methods”). The phosphorylating activity of PI3K toward its substrate L- α -phosphatidylinositol was analyzed by thin-layer chromatography and autoradiography. As shown in Fig. 3A, the activity of PI3K was increased following the Mn²⁺-induced activation of LFA-1 and subsequent cell adhesion onto ligand ICAM-1. Maximal activity was observed after 5 min (14-fold) and then decreased to almost basal levels after 30 min of LFA-1 activation. This increase in PI3K activity was dependent on the activation of LFA-1 as demonstrated by the fact that no enhanced activity was observed after 10 min of LFA-1-mediated T

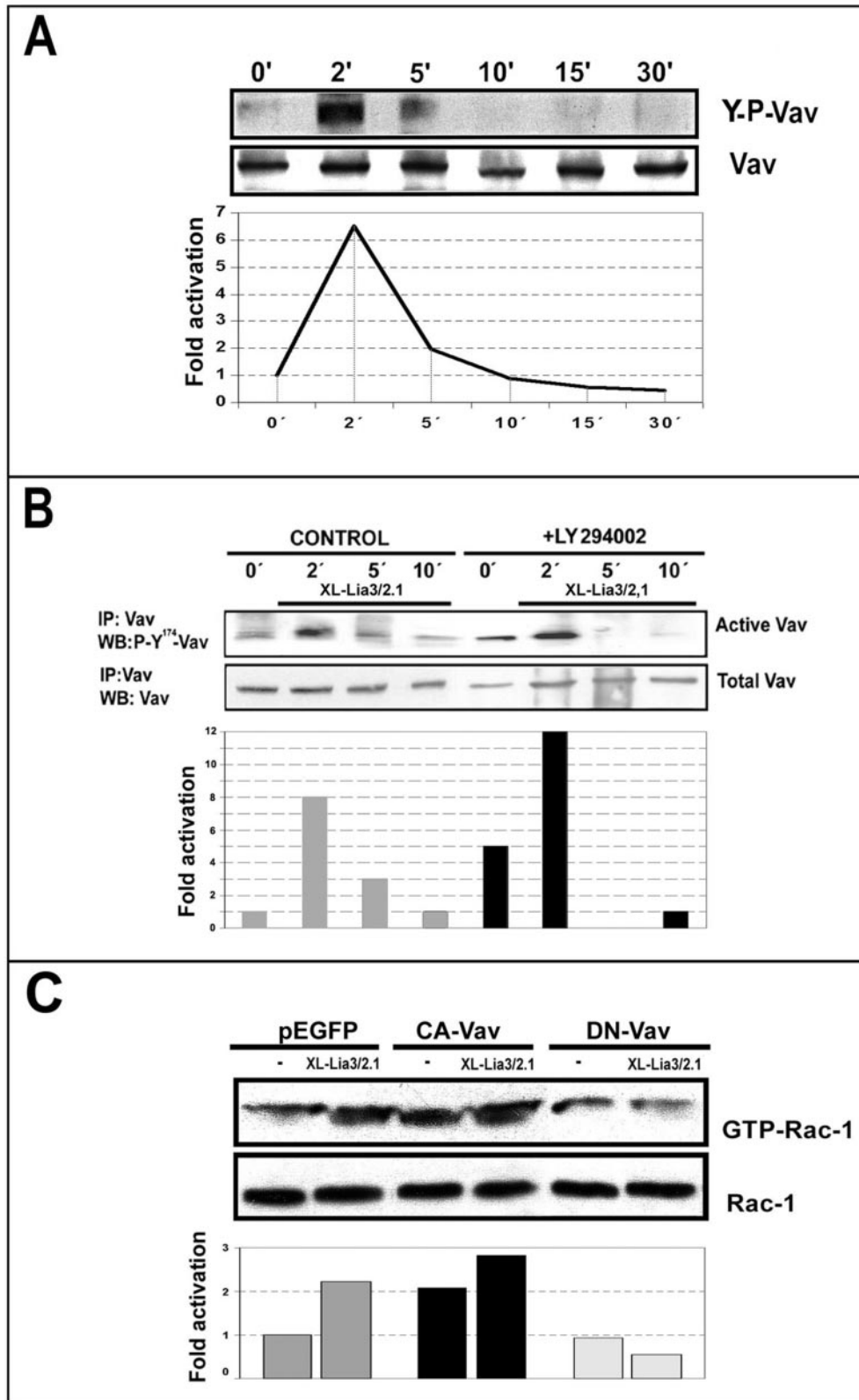
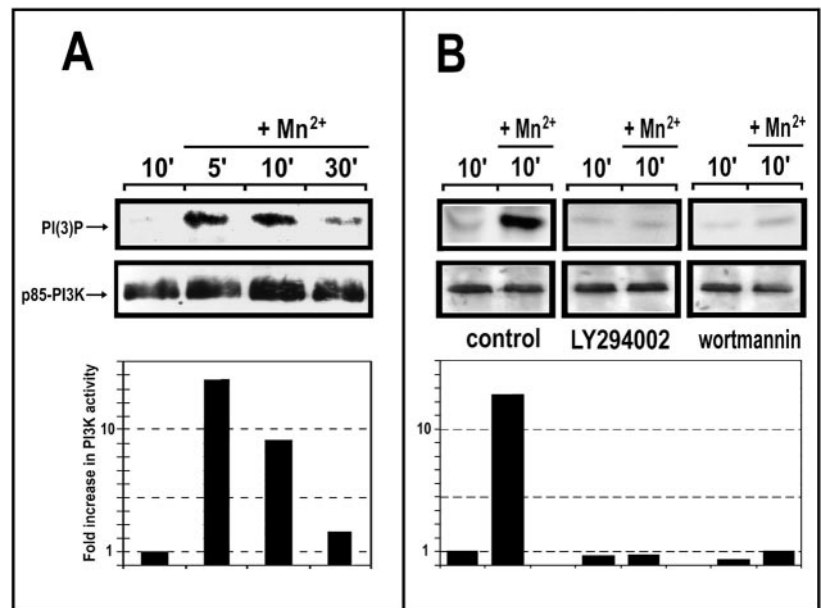


FIG. 2. LFA-1 activates Rac through a Vav-dependent pathway. *A*, HSB-2 T cells suspended in RPMI plus 20 mM Hepes were incubated with anti-LFA-1 mAb Lia3/2.1 (10 μ g/ml), and cross-linking of this antibody was induced as explained under "Materials and Methods" for different time periods. Cells were lysed, and Vav proteins from lysates were immunoprecipitated with anti-Vav antibody and immunoblotted with anti-phosphotyrosine (PY20) mAb (*upper panel*). Aliquots of total lysates were analyzed by Western blot (WB) with anti-Vav antibody to show equal loading (*lower panel*). -Fold activation of Vav over basal levels was quantified, and the kinetics of activation is represented. *B*, Vav activation was induced by cross-linking LFA-1 in HSB-2 T cells pretreated (+LY294002) or not (-) with the PI3K inhibitor LY294002 at 100 μ M and then cells were lysed in Buffer D, and Vav was immunoprecipitated (IP) (see "Materials and Methods"). Vav activation was detected by Western blot with the anti-phospho-Tyr¹⁷⁴-Vav antibody. Control load of total Vav is also shown. The level of activation of Vav was quantified and represented. *C*, transfected HSB-2 T cells with pEGFP, CA-Vav, and DN-Vav were used to perform pull-down assays as specified under "Materials and Methods." *Upper panel*, active Rac-1 (GTP-Rac-1) was detected by Western blot using the anti-Rac-1 antibody. *Lower panel*, total Rac-1 levels were analyzed by immunoblotting using aliquots of total lysates. Values of bars in *B* and *C* represent -fold activation with respect to basal levels.

FIG. 3. LFA-1 induces transient activation of PI3K. T lymphoblasts were allowed to adhere onto ICAM-1-coated dishes. *A, upper panel*, cells were stimulated with 200 μM Mn^{2+} for the indicated times and then lysed, PI3K was immunoprecipitated with a p85-specific antibody, and kinase activity was measured as described under "Materials and Methods." *Lower panel*, total PI3K levels were analyzed by immunoblotting using anti-p85 antibody. *B, upper panels*, T cells were pretreated for 30 min with PI3K inhibitors LY294002 (100 μM) or wortmannin (100 nM) before being stimulated or not with 200 μM Mn^{2+} for 10 min. *Lower panel*, total PI3K levels were analyzed by immunoblotting as in *A*. The quantification of the PI3K activity is represented in the *bar graphs* in *A* and *B*.



lymphocyte adhesion onto ligand ICAM-1 in the absence of Mn^{2+} (Fig. 3B) or following cell adhesion onto a nonspecific ligand poly-L-lysine (not shown). Similar results were obtained when activation of LFA-1 and adhesion of T lymphoblasts to ligand ICAM-1 was induced with mAb KIM-127 or when integrin LFA-1 was cross-linked with the specific anti-CD18 Lia3/2.1 mAb (not shown). Identical kinetics of PI3K activation was obtained with the human T cell line HSB-2 (not shown). Pretreatment of T lymphoblasts with the PI3K-specific inhibitors wortmannin (100 nM for 30 min) or LY294002 (100 μM for 30 min) completely abrogated the induction of activation of this lipid kinase after integrin LFA-1 engagement (Fig. 3B), confirming the specific detection of PI3K activity in these assays.

LFA-1 Induces Activation of Akt-1—As the kinase Akt-1 is a major PI3K effector (22, 23), we investigated its possible implication in the signaling pathway triggered by LFA-1. We analyzed the levels of the phosphorylated Akt-1 (active Akt-1 phosphorylated at Ser-473) by Western blot from lysates of T lymphoblasts treated with Mn^{2+} and allowed to adhere onto ICAM-1-coated dishes for various time periods. As shown in Fig. 4A, an increase in Akt-1 phosphorylation was evident 10 min after Mn^{2+} -induced LFA-1-activation, remaining still high after 60 min. This activation of Akt-1 was completely dependent on PI3K, because it was abrogated by preincubating the cells with the PI3K inhibitor LY294002 (Fig. 4B), confirming the upstream position of PI3K relative to Akt-1 in this signaling pathway. When the interaction of LFA-1 integrin with its ligand ICAM-1 was prevented by using the blocking anti-LFA-1 mAb Lia3/2.1 no activation of Akt-1 was observed, clearly demonstrating its dependence on LFA-1 (Fig. 4B). A similar kinetics of activation of Akt-1 following cross-linking of LFA-1 was observed with the T cell line HSB-2 (see Fig. 5).

The PI3K/Akt-1 Axis Is a Negative Regulator of LFA-1-mediated Rac-1 Activity—To demonstrate the involvement of the PI3K/Akt-1 axis in the control of Rac-1 activity following LFA-1 engagement, T cells were pretreated with the PI3K inhibitor LY294002, and the activity levels of Rac-1 were analyzed at different times after cross-linking of LFA-1. Interestingly, under these conditions of inhibition of PI3K the activation of Rac-1 was no longer transient, but it was converted into a more stable activation kinetics. As shown in Fig. 5 (upper panel), in T cells treated with LY294002 the Rac-1 activation phase was similar, and maximal levels of GTP-Rac-1 were also observed

10 min after LFA-1 activation as in control untreated cells. However, the subsequent return to basal levels of Rac-1 activity that was observed at longer times in control cells was prevented. Under the same conditions, LY294002 caused a blockade of Akt-1 activation (Fig. 5, lower panel), demonstrating that the PI3K/Akt-1 was inhibited by this compound. These results indicate that PI3K behaves as an inhibitory molecule acting upstream of Rac-1 in the LFA-1 signaling pathway. To directly test the involvement of Akt-1 in the control by PI3K of Rac-1 activity, we transiently transfected the HSB-2 T cell line with cDNA constructs coding for constitutively active or dominant-negative forms of Akt-1 (CA-Akt-1 and DN-Akt-1; both fused to EGFP). Fig. 6A shows that transfection of HSB-2 T cells with CA-Akt-1 resulted in lower levels of active Rac-1 compared with cells transfected with DNA control plasmid (pEGFP), whereas the levels of active Rac-1 (GTP-Rac-1) were elevated in HSB-2 T cells transfected with DN-Akt-1. These results demonstrate that in T cells Akt-1 exerts an inhibitory effect on the activity of Rac-1. Accordingly, it has been reported (51) that *in vitro* Akt-mediated phosphorylation of Ser⁷⁴-Rac leads to its inactivation. To test this point with intact cells, we have examined Rac phosphorylation in HSB-2 T cells transfected with CA-Akt-1. Using two different antibodies, a general anti-phospho-serine antibody (not shown) and also a specific antibody that detects the consensus sequence (RLRPLpS/pT) that is phosphorylated specifically by Akt-1, we have not detected an increase in Rac phosphorylation (Fig. 6B). As a control we used Bad, a well established substrate of Akt-1, which was readily phosphorylated by CA-Akt-1 (not shown). Taken together, the data indicate that PI3K/Akt-1 is responsible for the decline and return to basal levels of activity of the Rac-1 GTPase observed at 20 min after induction of LFA-1 activation by a mechanism that *in vivo* does not seem to involve a direct Akt-1 phosphorylation of Rac (see Figs. 5, 6, and 8).

Transient Activation of Rac-1 Is Required for T Cell Polarization and Migration on ICAM-1—The results presented above demonstrate that activation of LFA-1 on T cells triggers two signaling pathways involving Vav and PI3K/Akt-1 that control the activity of Rac-1. To directly confirm that Rac-1 activity plays an essential role in the control of T cell morphology and motility, we obtained HSB-2 T cells with sustained enhanced Rac-1 activity by overexpressing either CA-Vav or CA-Rac-1 constructs. Transfected cells were plated on ICAM-1,

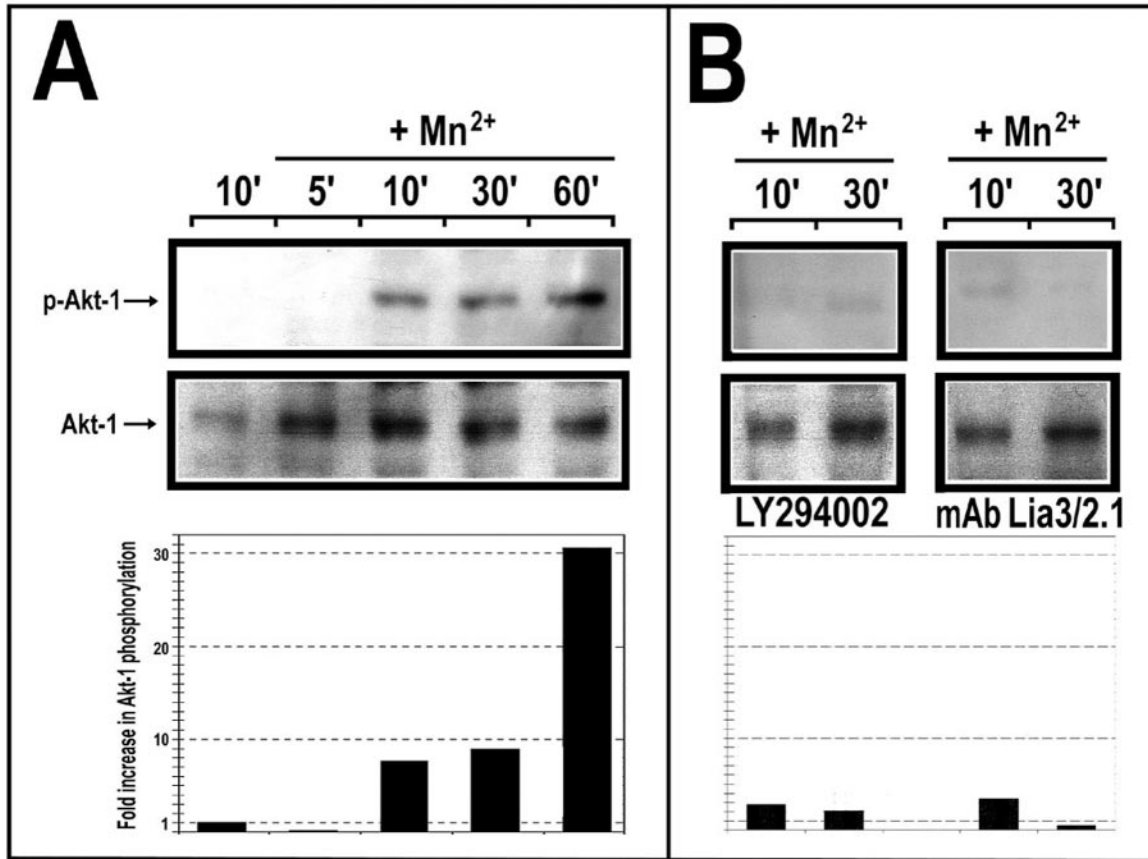


FIG. 4. **LFA-1 induces activation of Akt-1 in T cells.** *A*, time course of LFA-1-stimulated Akt-1 activity. T lymphoblasts were plated onto ICAM-1-coated dishes, stimulated with 200 μM MnCl_2 for several time periods, lysed, and subjected to Western blotting. Active Akt-1 was detected with anti-phospho-Akt-1 (*upper panels*). Total levels of Akt-1 were analyzed with anti-Akt-1 antibody (*lower panels*). The -fold increase in Akt-1 activity is also quantified. *B*, T cells were pretreated for 30 min with either the PI3K inhibitor LY294002 (100 μM) or with the anti-LFA-1 mAb LIA 3/2.1 (10 $\mu\text{g}/\text{ml}$) to prevent the interaction between LFA-1 and ICAM-1 (not shown). Cells were stimulated for the indicated times with 200 μM MnCl_2 , and active and total Akt-1 was determined as in *A*.

and LFA-1 was activated with the stimulatory antibody KIM-127 (or with Mn^{2+} ; not shown). As shown in Fig. 7A the morphological elongation (and also the motility; not shown) of T cells was completely blocked in these transfected HSB-2 cells, whereas in cells transfected with control vector pEGFP no such inhibition was observed (not shown). In addition, as the inhibition of the PI3K/Akt-1 signaling pathway with LY294002 blocks the inactivation phase and results in sustained activation of Rac-1 (see Figs. 5 and 6) we expected that this inhibition of PI3K should also result in inhibition of T cell polarization. As shown in Fig. 7B, treatment of T lymphoblasts (or HSB-2 T cells; data not shown) with the PI3K inhibitors LY294002 (or wortmannin; not shown) prior to the induction of activation of integrin LFA-1 (either with Mn^{2+} or with the specific stimulatory anti-CD18 mAb KIM-127) completely abrogated the acquisition of the elongated polarized T cell morphology on ICAM-1. As we have demonstrated before, LFA-1 induces activation of the tyrosine kinase PYK-2 in T cells (17–19), and this activation was completely dependent on changes in T cell morphology; therefore we also expected that inhibition of changes in morphology because of PI3K inhibition and concomitant Rac-1 sustained activation would also block LFA-1-dependent activation of PYK-2. As shown in Fig. 7C, treatment of the cells with the PI3K inhibitor abrogated the activation of PYK-2. Taken together, these results demonstrate that inactivation of Rac-1 is required for LFA-1-dependent cell polarization and motility in T cells.

DISCUSSION

The leukocyte integrin LFA-1 mediates the adhesive interactions of T lymphocytes with endothelial cells during chemokine-directed extravasation into inflammatory foci and with antigen presenting cells during the initiation of an immune response. It has been shown that LFA-1 can transmit multiple intracellular signals in different types of leukocytes, including T cells (12, 13, 15–18). We and others have shown before that upon activation of LFA-1 and subsequent ligand engagement dramatic changes in T cell morphology take place that are associated with alterations in the organization of the actin cytoskeleton (13, 17). As the GTPase Rac-1 is a key regulatory molecule for actin cytoskeletal organization, we decided to study whether LFA-1 was able to induce activation of this GTPase in T cells. Herein we show that LFA-1 induces a potent and transient activation of Rac-1. Maximal Rac-1 activity is reached 10 min after the induction of LFA-1 activation and then declines to basal levels at longer times. This transient stimulation of Rac-1 activity was observed using three different methods for activation of LFA-1: (i) addition of Mn^{2+} , (ii) clustering the LFA-1 molecules, and (iii) direct stimulation with activating mAbs. The transient Rac-1 stimulation suggests that distinct signals are regulating this small GTPase. When we analyzed the signaling molecules that could account for this transient behavior of Rac-1 activity, we found that Vav and PI3K/Akt-1 play an important role. Furthermore, by using constitutively active

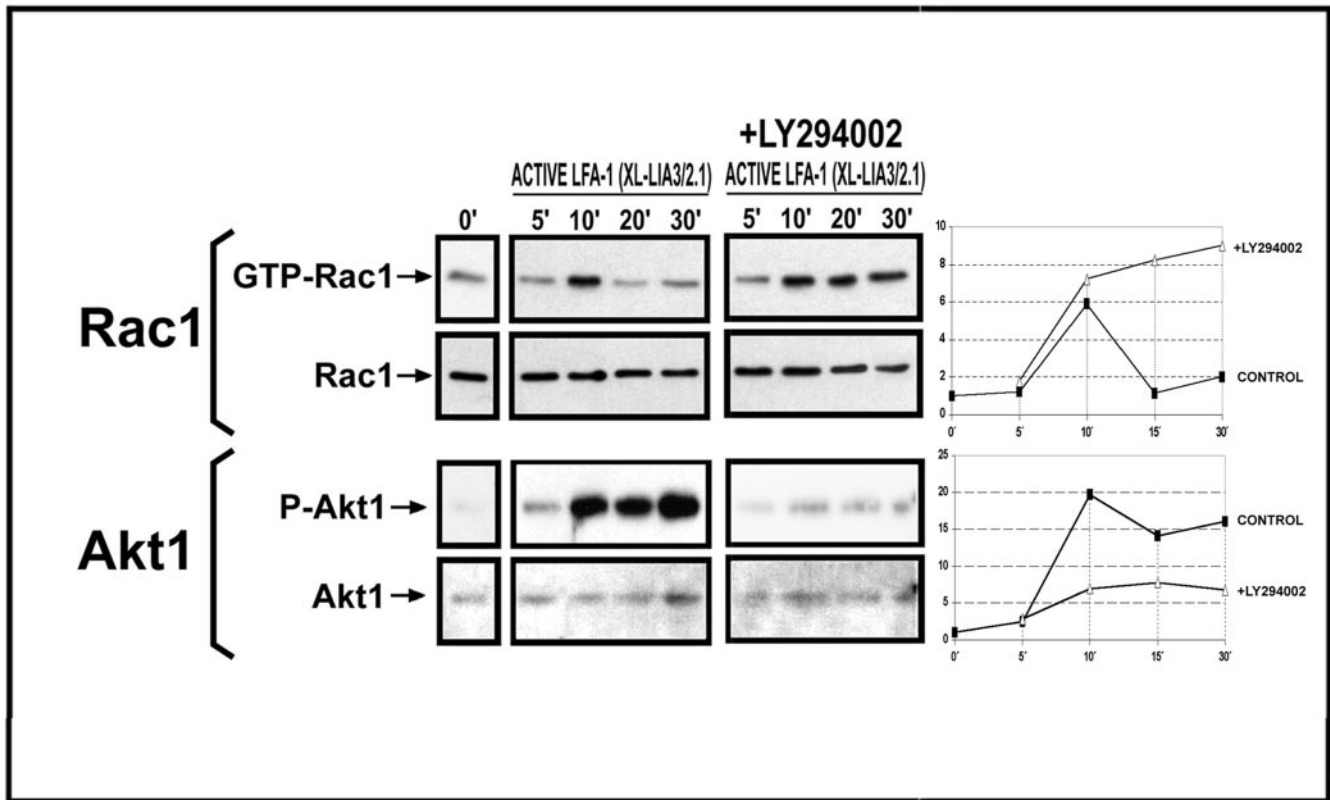


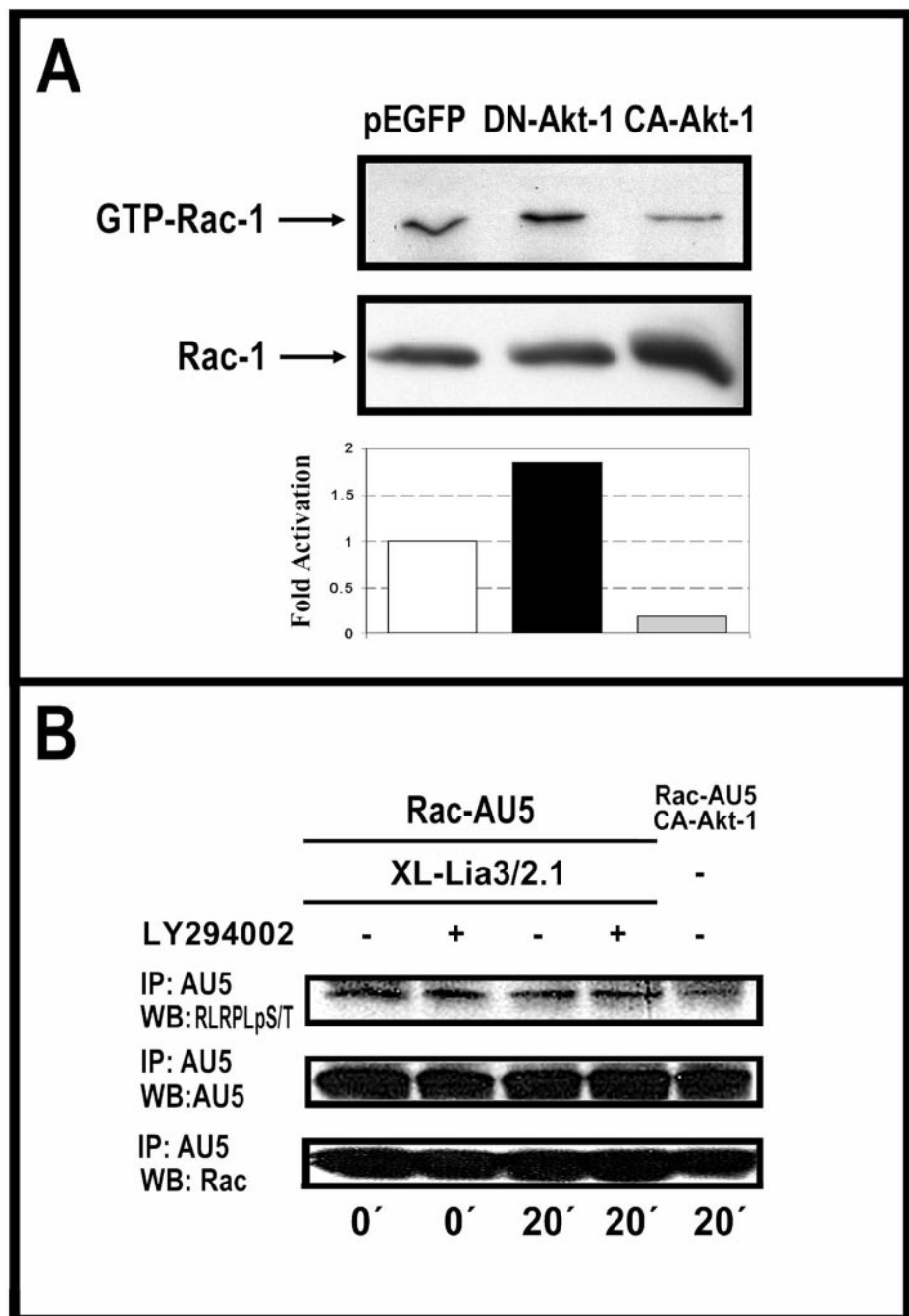
FIG. 5. LFA-1 modulates Rac-1 activity through PI3K. The kinetics of Rac-1 activation mediated by LFA-1 was compared in HSB-2 T cells untreated or pretreated with 100 μ M PI3K inhibitor LY294002 for 30 min. LFA-1 was then induced by inducing clustering of the integrin for the indicated times with the anti LFA-1 mAb LIA3/2.1 (see "Materials and Methods"). The active Rac-1 fraction from lysates (*GTP-Rac-1*; upper panel) was pulled down with GST-PAK-CRIB, fractionated by SDS-PAGE, and immunoblotted using anti-Rac-1 antibody. Total Rac-1 (*Rac-1*; lower panel) was analyzed in fractions of total lysates reserved for loading controls and detected by Western blotting with anti-Rac-1 antibody. The -fold activation increased was quantified, and the Rac-1 kinetics is represented on the right of the panels. The kinetics of Akt-1 activation in this experiment, obtained as in Fig. 4A using anti-Akt-1-phospho-Ser polyclonal antibody (*Akt-1*; upper left panel), and the anti-total Akt-1 antibody (*Akt-1*; lower left panel) are also included. The inhibition of the PI3K/Akt-1 signaling in T cells pretreated with LY294002 (100 μ M) is shown in Akt-1 right panels. The Akt-1 -fold activation was quantified and graphically represented on the right of the Akt-1 panels.

and dominant-negative mutants of these molecules and pharmacological inhibitors, we provide evidence that Vav and PI3K/Akt-1 play opposing roles on the regulation of the activity of Rac-1, controlling the activation and inactivation phases of Rac-1 activity, respectively. In line with previous observations (37) in other lymphocyte systems, our findings also indicate that in the context of LFA-1 signaling, Vav activation is independent of the PI3K activity, because inhibition of this enzyme does not affect the activity of this GEF (Fig. 2). Our experimental data are integrated in the model presented in Fig. 8, which is based on the following points. First, the observed time courses of the LFA-1-mediated changes in the activity of Vav and PI3K/Akt-1 are consistent with the postulated activating/inhibitory effects exerted on Rac-1 by Vav and Akt-1, respectively (see Figs. 1–5). Second, overexpression of constitutively active and dominant-negative forms of Vav induce activation and abrogation of LFA-1-mediated Rac-1 activation, respectively (Fig. 2). Third, inhibition of PI3K did not affect Vav activation (Fig. 2). Fourth, transfection with a constitutively active form of Akt-1 blunted Rac-1 activity, and overexpression of dominant-negative Akt-1 mutant induced activation of Rac-1 (Fig. 6). Fifth, pre-treatment of the cells with the PI3K inhibitors LY294002 or wortmannin prevented the decline in the activity of Rac-1 (Fig. 5).

In contrast to Vav, which, because of its GEF activity, induces Rac activation, the mechanism whereby PI3K/Akt inhibits Rac is presently unclear. Because phosphorylation by Akt

usually leads to inhibition of the substrate function, we analyzed the possibility that the observed inhibition of the Rac-1 activity might be a result of Akt-mediated Rac-1 phosphorylation. Rac-1 and other members of the small G protein family, including Cdc42 and RhoA, possess a Ser residue preceded by arginines that resemble the consensus sequence for Akt substrates (RLRPLSY). However, according to the algorithm developed by Yaffe *et al.* (52), this sequence is unlikely to be actually phosphorylated by Akt *in vivo*, because it has a worse score (0.3192) when compared with well established substrates such as BAD (0.1775), GSK3 (0.1697), FOXO3a (0.1174), or eNOS (0.2032). Moreover, the crystal structure of Rac-1, described by Hirshberg *et al.* (53), further indicates that this Ser is not exposed on the surface of this small GTPase, therefore making difficult its accessibility to Akt-1. In agreement with these predictions, we could not detect a difference in the pattern of Rac-1 phosphorylation in cells transfected with constitutively active Akt-1 or treated with the PI3K inhibitor LY294002 (Fig. 6). Our data are in contrast with a previous study (51) that reported the direct phosphorylation of Rac-1 by Akt. The discrepancy with our results might be explained in part by the fact that this previous study was performed using Akt *in vitro* kinase assays with Rac-1-derived fluorescent peptides as substrates. If direct phosphorylation/inhibition by Akt-1 does not seem to be the key event, then other mechanisms must be invoked to account for the observed LFA-1-dependent inhibition of Rac-1 activity. One such alternative mechanism involving the participation of a Rac-1-GTPase-ac-

FIG. 6. Akt-1 inactivates Rac-1. *A*, the T cell line HSB-2 was transfected with EGFP-vector cDNA, DN-Akt-1, and CA-Akt-1. After 24 h of electroporation, cells were washed twice in RPMI medium and lysed as explained under "Materials and Methods." The active Rac-1 fraction from total lysates (*GTP-Rac-1*; upper panel) was pulled down with GST-PAK-CRIB, fractionated by SDS-PAGE, and immunoblotted using an anti-Rac-1 antibody. Total Rac-1 (*Rac-1*; lower panel) was analyzed in fractions of total lysates reserved for loading controls and detected by Western blotting (WB) with anti-Rac-1. The quantification of active Rac-1, referred to as control pEGFP-transfected cells, is represented in the graph below the panels. *B*, HSB-2 T cells transfected with tagged Rac-AU5 cDNA pretreated (+) or not (-) with the PI3K inhibitor LY294002 at 100 μ M and cells co-transfected with CA-Akt-1 and tagged Rac-AU5 cDNAs were starved for 2 h. After this period, LFA-1 activation was induced by cross-linking (*XL-Lia3/2.1*). All the cells were lysed in Buffer E, and cleared lysates were incubated with anti-AU5 mAb to precipitate tagged Rac-AU5. Immunoprecipitates (IP) were fractionated by SDS-PAGE and immunoblotted with an antibody that specifically recognizes the consensus sequence (RLRPLpS/pT) phosphorylated by Akt-1. The total Rac-AU5 and total Rac was detected in the last two panels.



tivating protein has been published very recently (54). Further studies will be required to elucidate this possibility in the context of LFA-1 signaling in T cells.

We have also observed that maintaining the activity of Rac at high levels, by overexpressing constitutively active forms of Rac or Vav or by pharmacologically inhibiting PI3K/Akt, blocked the LFA-1-dependent changes in morphology and the motility of T cells. It has been observed before that the effects of active Rac on cell morphology and motility depend on the cellular system analyzed, with examples where active Rac either stimulates or inhibits cell motility (31, 55, 56). How could active Rac lead to the blockade of T cell motility and morphology? We speculate that constitutively active Rac might exert its effects by disruption of the fine temporal regulation of the organization of the actin cytoskeleton. Rac possesses several downstream effectors (26, 28), including the phosphatidylinositol phosphate 5-kinase, an enzyme that

catalyzes the conversion of phosphatidylinositol 4-phosphate to phosphatidylinositol 4,5-bisphosphate, and the serine/threonine kinase PAK, a well established Rac effector that regulates several downstream components. Together, both enzymes regulate important cytoskeletal processes. The product of phosphatidylinositol phosphate 5-kinase, phosphatidylinositol 4,5-bisphosphate, has an important role in the regulation of the cytoskeleton and the interaction between the cytoskeleton and the membrane (57). On the other hand, PAK may regulate several cytoskeletal proteins (*e.g.* filamin) or regulators of the cytoskeleton, like cofilin (58, 59). In particular, cofilin participates in the cycle or severing of actin fibers that are subsequently polymerized by Arp2/3 and formins (60, 61). This process of actin depolymerization/polymerization is cyclical. It could be possible that by maintaining Rac in an activated state the cyclical changes that lead to variations in cell morphology and motility are altered.

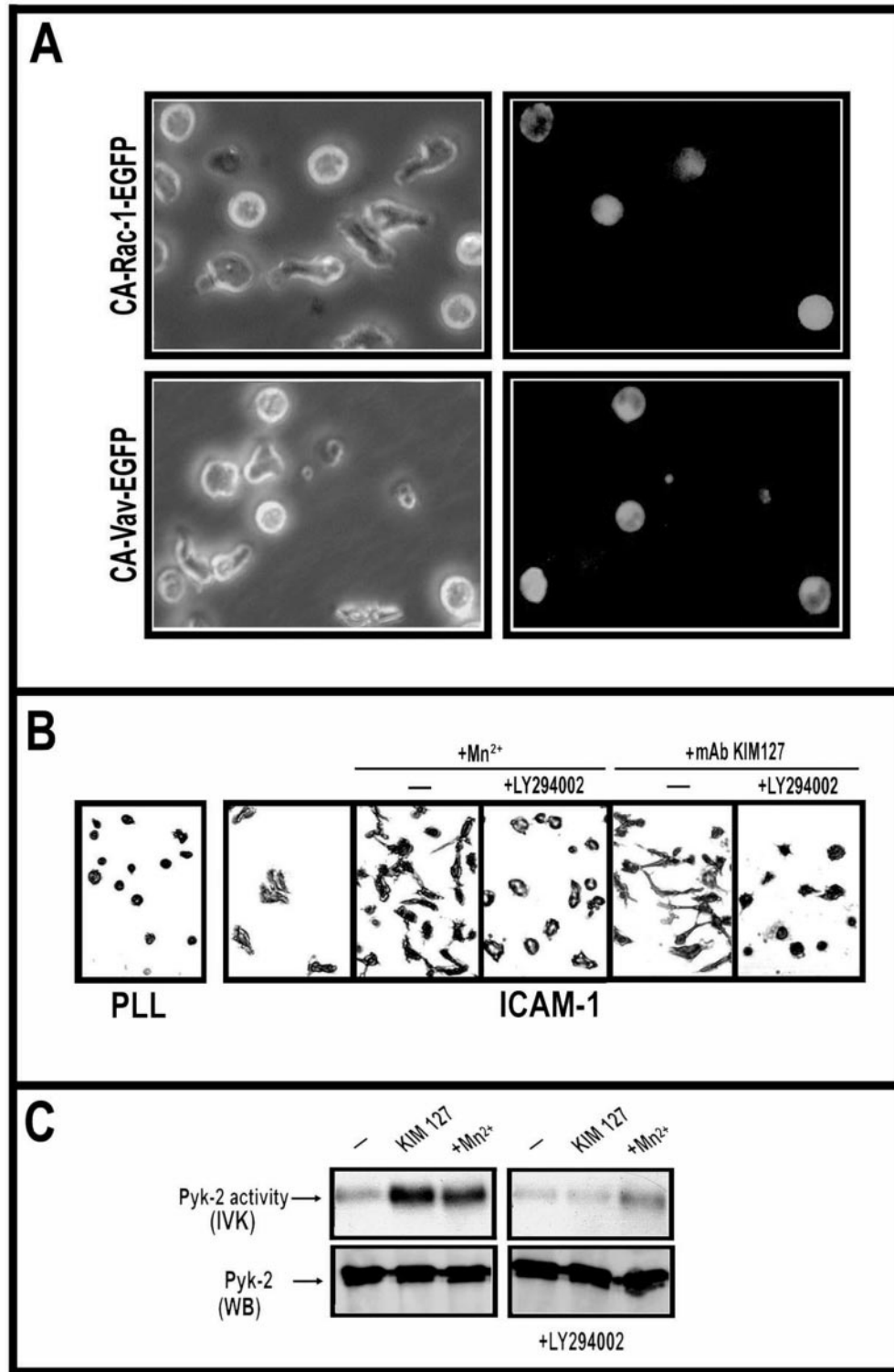


FIG. 7. Role of PI3K/Akt and Rac-1 signaling in adhesion, polarization, migration, and activation of PYK-2 in T cells. *A*, transfection of constitutively active Rac-1 and Vav blocks LFA-1-dependent cell polarization. HSB-2 T cells were transiently transfected with CA-Vav cDNA and CA-Rac-1. After 16–24 h, cells were starved for 90 min in 20 mM Hepes-RPMI 1640 medium and, after this period, plated onto ICAM-1-coated dishes and LFA-1 stimulated with the mAb KIM-127 anti-CD18 and recorded by time-lapse videomicroscopy; the frames shown correspond to a time point of 90 min after the contact between cells and ligand ICAM-1. The phase contrast (*left*) and fluorescence (*right*) images showing transfected cells are shown. *B*, inhibition of PI3K blocks LFA-1-dependent cell polarization. T lymphoblasts were either pretreated for 30 min with the PI3K inhibitor LY294002 (100 μ M) or not pretreated before allowing them to adhere on poly-L-lysine or ICAM-1-coated plastic wells for 60 min at 37 $^{\circ}$ C. LFA-1 activation was induced with either Mn²⁺ (200 μ M) or anti-CD18 stimulatory mAb KIM-127 (10 μ g/ml). Non-adherent T lymphoblasts were washed, and adherent cells were fixed, permeabilized, stained, and photographed. *C*, LFA-1-induced activation of tyrosine kinase PYK-2 is blocked by PI3K inhibition. T lymphoblasts were either pretreated for 30 min with the PI3K inhibitor LY294002 (100 μ M) or not treated before plating them on ICAM-1-coated plastic dishes for 40 min at 37 $^{\circ}$ C. LFA-1 activation was induced with either Mn²⁺ (200 μ M) or anti-CD18 stimulatory mAb KIM-127 (10 μ g/ml). After this period, all T cells in the dishes were lysed, PYK-2 was immunoprecipitated with specific antibodies, and *in vitro* autophosphorylation kinase activity was measured. Parallel control samples were run to show equal loading by Western blot (WB).

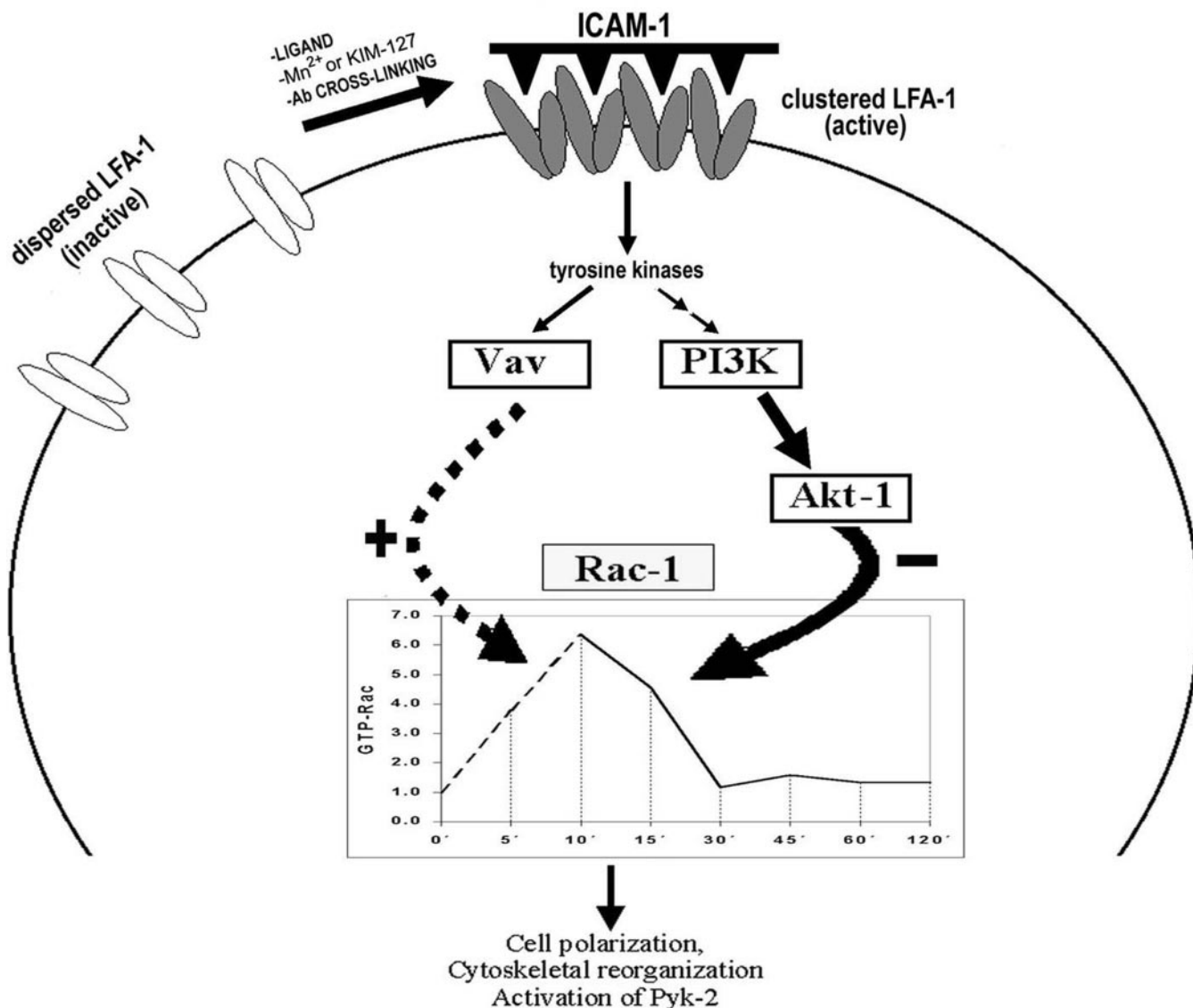


FIG. 8. **Model for Rac-1 regulation by LFA-1 signaling.** LFA-1 activation induced by divalent cations, specific activating mAbs, cross-linking antibodies, or higher ligand concentrations triggers two signaling pathways through the small GTPase Rac-1. The first pathway involves the early activation of tyrosine kinases and subsequent activation of the Rac-GEF Vav (62, 63) and leads to Rac-1 activation. The second route is a novel Rac-1 inactivation signaling pathway, in which LFA-1 triggers the activation of tyrosine kinases and subsequent binding of the p85 regulatory subunit of the PI3K to phosphorylated proteins. Activated PI3K stimulates the activity of its downstream effector, the Ser-Thr kinase Akt-1, which leads indirectly to the inactivation of Rac-1. Through the transient regulation of Rac-1 activity by the sequential activation of different signaling molecules the integrin LFA-1 exerts a spatio-temporal control on cytoskeletal organization, morphological changes, and motility of T cells.

Activated Rac, acting through PAK, by "freezing" cofilin in a phosphorylated/inactive conformation, may unbalance the process leading to changes in morphology and cell motility. Therefore it could be possible that Rac activity must be temporally regulated in the cycle of activation and inactivation, and disruption of this process may lead to dramatic effects on morphology and motility. Taken together, our results demonstrate an important role for Vav and PI3K/Akt-1 in the LFA-1 signaling pathway that temporally controls in T cells the activity of Rac-1 and changes in cell morphology and motility.

REFERENCES

- Sanchez-Madrid, F., and del Pozo, M. A. (1999) *EMBO J.* **18**, 501–511
- Serrador, J. M., Nieto, M., and Sanchez-Madrid, F. (1999) *Trends Cell Biol.* **9**, 228–233
- Bromley, S. K., Burack, W. R., Johnson, K. G., Somersalo, K., Sims, T. N., Sumen, C., Davis, M. M., Shaw, A. S., Allen, P. M., and Dustin, M. L. (2001) *Annu. Rev. Immunol.* **19**, 375–396
- Harris, E. S., McIntyre, T. M., Prescott, S. M., and Zimmerman, G. A. (2000) *J. Biol. Chem.* **275**, 23409–23412
- Gahmberg, C. G., Valmu, L., Fagerholm, S., Kotovuori, P., Ihanus, E., Tian, L., and Pessa-Morikawa, T. (1998) *Cell. Mol. Life Sci.* **54**, 549–555
- Campbell, J. J., Hedrick, J., Zlotnik, A., Siani, M. A., Thompson, D. A., and Butcher, E. C. (1998) *Science* **279**, 381–384
- Dustin, M. L., and Springer, T. A. (1989) *Nature* **341**, 619–624
- van Kooyk, Y., van de Wiel-van Kemenade, P., Weder, P., Kuijpers, T. W., and Figdor, C. G. (1989) *Nature* **342**, 811–813
- Dransfield, I., Cabanas, C., Craig, A., and Hogg, N. (1992) *J. Cell Biol.* **116**, 219–226
- Stephens, P., Romer, J. T., Spitali, M., Shock, A., Ortlepp, S., Figdor, C. G., and Robinson, M. K. (1995) *Cell Adhes. Commun.* **3**, 375–384
- Ortlepp, S., Stephens, P. E., Hogg, N., Figdor, C. G., and Robinson, M. K. (1995) *Eur. J. Immunol.* **25**, 637–643
- Petruzzelli, L., Takami, M., and Herrera, R. (1996) *J. Biol. Chem.* **271**, 7796–7801
- Porter, J. C., Bracke, M., Smith, A., Davies, D., and Hogg, N. (2002) *J. Immunol.* **168**, 6330–6335
- Wacholtz, M. C., Patel, S. S., and Lipsky, P. E. (1989) *J. Exp. Med.* **170**, 431–448
- Kanner, S. B., Grosmaire, L. S., Ledbetter, J. A., and Damle, N. K. (1993) *Proc. Natl. Acad. Sci. U. S. A.* **90**, 7099–7103
- Arroyo, A. G., Campanero, M. R., Sanchez-Mateos, P., Zapata, J. M., Ursa, M. A., del Pozo, M. A., and Sanchez-Madrid, F. (1994) *J. Cell Biol.* **126**, 1277–1286
- Rodriguez-Fernandez, J. L., Gomez, M., Luque, A., Hogg, N., Sanchez-Madrid, F., and Cabanas, C. (1999) *Mol. Biol. Cell* **10**, 1891–1907
- Rodriguez-Fernandez, J. L., Sanchez-Martin, L., Rey, M., Vicente-

- Manzanares, M., Narumiya, S., Teixido, J., Sanchez-Madrid, F., and Cabanas, C. (2001) *J. Biol. Chem.* **276**, 40518–40527
19. Rodriguez-Fernandez, J. L., Sanchez-Martin, L., de Frutos, C. A., Sancho, D., Robinson, M., Sanchez-Madrid, F., and Cabanas, C. (2002) *J. Leukocyte Biol.* **71**, 520–530
 20. Vicente-Manzanares, M., Rey, M., Jones, D. R., Sancho, D., Mellado, M., Rodriguez-Frade, J. M., del Pozo, M. A., Yanez-Mo, M., de Ana, A. M., Martinez, A. C., Merida, I., and Sanchez-Madrid, F. (1999) *J. Immunol.* **163**, 4001–4012
 21. Niggli, V., and Keller, H. (1997) *Eur. J. Pharmacol.* **335**, 43–52
 22. Cantley, L. C. (2002) *Science* **296**, 1655–1657
 23. Leegers, S. J., Vanhaesebroeck, B., and Waterfield, M. D. (1999) *Curr. Opin. Cell Biol.* **11**, 219–225
 24. Heit, B., Tavener, S., Raharjo, E., and Kubes, P. (2002) *J. Cell Biol.* **159**, 91–102
 25. Ridley, A. J. (2001) *J. Cell Sci.* **114**, 2713–2722
 26. Bishop, A. L., and Hall, A. (2000) *Biochem. J.* **348**, 241–255
 27. Symons, M., and Settleman, J. (2000) *Trends Cell Biol.* **10**, 415–419
 28. Takai, Y., Sasaki, T., and Matozaki, T. (2001) *Physiol. Rev.* **81**, 153–208
 29. Vicente-Manzanares, M., and Sanchez-Madrid, F. (2004) *Nat. Rev. Immunol.* **4**, 110–122
 30. D'Souza-Schorey, C., Boettner, B., and Van Aelst, L. (1998) *Mol. Cell. Biol.* **18**, 3936–3946
 31. del Pozo, M. A., Vicente-Manzanares, M., Tejedor, R., Serrador, J. M., and Sanchez-Madrid, F. (1999) *Eur. J. Immunol.* **29**, 3609–3620
 32. Ridley, A. J. (2001) *FEBS Lett.* **498**, 168–171
 33. Jones, G. E., Allen, W. E., and Ridley, A. J. (1998) *Cell Adhes Commun* **6**, 237–245
 34. Fischer, K. D., Kong, Y. Y., Nishina, H., Tedford, K., Marengere, L. E., Koziaradzki, I., Sasaki, T., Starr, M., Chan, G., Gardener, S., Nghiem, M. P., Bouchard, D., Barbacid, M., Bernstein, A., and Penninger, J. M. (1998) *Curr. Biol.* **8**, 554–562
 35. Han, J., Luby-Phelps, K., Das, B., Shu, X., Xia, Y., Mosteller, R. D., Krishna, U. M., Falck, J. R., White, M. A., and Broek, D. (1998) *Science* **279**, 558–560
 36. Bustelo, X. R. (2000) *Mol. Cell. Biol.* **20**, 1461–1477
 37. Zugaza, J. L., Lopez-Lago, M. A., Caloca, M. J., Dosil, M., Movilla, N., and Bustelo, X. R. (2002) *J. Biol. Chem.* **277**, 45377–45392
 38. Berendt, A. R., McDowall, A., Craig, A. G., Bates, P. A., Sternberg, M. J., Marsh, K., Newbold, C. I., and Hogg, N. (1992) *Cell* **68**, 71–81
 39. del Pozo, M. A., Sanchez-Mateos, P., Nieto, M., and Sanchez-Madrid, F. (1995) *J. Cell Biol.* **131**, 495–508
 40. Robinson, M. K., Andrew, D., Rosen, H., Brown, D., Ortlepp, S., Stephens, P., and Butcher, E. C. (1992) *J. Immunol.* **148**, 1080–1085
 41. Lopez-Lago, M., Lee, H., Cruz, C., Movilla, N., and Bustelo, X. R. (2000) *Mol. Cell. Biol.* **20**, 1678–1691
 42. del Peso, L., Gonzalez-Garcia, M., Page, C., Herrera, R., and Nunez, G. (1997) *Science* **278**, 687–689
 43. Murga, C., Zohar, M., Teramoto, H., and Gutkind, J. S. (2002) *Oncogene* **21**, 207–216
 44. Salinas, M., Martin, D., Alvarez, A., and Cuadrado, A. (2001) *Mol. Cell. Neurosci.* **17**, 67–77
 45. Martin, D., Salinas, M., Fujita, N., Tsuruo, T., and Cuadrado, A. (2002) *J. Biol. Chem.* **277**, 42943–42952
 46. Shaw, L. M., Rabinovitz, I., Wang, H. H., Tokar, A., and Mercurio, A. M. (1997) *Cell* **91**, 949–960
 47. Sander, E. E., ten Klooster, J. P., van Delft, S., van der Kammen, R. A., and Collard, J. G. (1999) *J. Cell Biol.* **147**, 1009–1022
 48. del Pozo, M. A., Schwartz, M. A., Hu, J., Kiesses, W. B., Altman, A., and Villalba, M. (2003) *J. Immunol.* **170**, 41–47
 49. Zheng, L., Sjolander, A., Eckerdal, J., and Andersson, T. (1996) *Proc. Natl. Acad. Sci. U. S. A.* **93**, 8431–8436
 50. Aghazadeh, B., Lowry, W. E., Huang, X. Y., and Rosen, M. K. (2000) *Cell* **102**, 625–633
 51. Kwon, T., Kwon, D. Y., Chun, J., Kim, J. H., and Kang, S. S. (2000) *J. Biol. Chem.* **275**, 423–428
 52. Yaffe, M. B., Lepar, G. G., Lai, J., Obata, T., Volinia, S., and Cantley, L. C. (2001) *Nat. Biotechnol.* **19**, 348–353
 53. Hirshberg, M., Stockley, R. W., Dodson, G., and Webb, M. R. (1997) *Nat. Struct. Biol.* **4**, 147–152
 54. Dib, K., Melander, F., Axelsson, L., Dagher, M. C., Aspenstrom, P., and Andersson, T. (2003) *J. Biol. Chem.* **278**, 24181–24188
 55. Stam, J. C., Michiels, F., van der Kammen, R. A., Moolenaar, W. H., and Collard, J. G. (1998) *EMBO J.* **17**, 4066–4074
 56. Allen, W. E., Zicha, D., Ridley, A. J., and Jones, G. E. (1998) *J. Cell Biol.* **141**, 1147–1157
 57. Raucher, D., Stauffer, T., Chen, W., Shen, K., Guo, S., York, J. D., Sheetz, M. P., and Meyer, T. (2000) *Cell* **100**, 221–228
 58. Vadlamudi, R. K., Li, F., Adam, L., Nguyen, D., Ohta, Y., Stossel, T. P., and Kumar, R. (2002) *Nat. Cell Biol.* **4**, 681–690
 59. Nishita, M., Aizawa, H., and Mizuno, K. (2002) *Mol. Cell. Biol.* **22**, 774–783
 60. Miletic, A. V., Swat, M., Fujikawa, K., and Swat, W. (2003) *Curr. Opin. Immunol.* **15**, 261–268
 61. Evangelista, M., Zigmund, S., and Boone, C. (2003) *J. Cell Sci.* **116**, 2603–2611
 62. Miranti, C. K., Leng, L., Maschberger, P., Brugge, J. S., and Shattil, S. J. (1998) *Curr. Biol.* **8**, 1289–1299
 63. Deckert, M., Tartare-Deckert, S., Couture, C., Mustelin, T., and Altman, A. (1996) *Immunity* **5**, 591–604

Signaling through the Leukocyte Integrin LFA-1 in T Cells Induces a Transient Activation of Rac-1 That Is Regulated by Vav and PI3K/Akt-1

Lorena Sánchez-Martín, Noelia Sánchez-Sánchez, M. Dolores Gutiérrez-López, Ana I. Rojo, Miguel Vicente-Manzanares, María José Pérez-Alvarez, Paloma Sánchez-Mateos, Xosé R. Bustelo, Antonio Cuadrado, Francisco Sánchez-Madrid, José Luis Rodríguez-Fernández and Carlos Cabañas

J. Biol. Chem. 2004, 279:16194-16205.

doi: 10.1074/jbc.M400905200 originally published online February 11, 2004

Access the most updated version of this article at doi: [10.1074/jbc.M400905200](https://doi.org/10.1074/jbc.M400905200)

Alerts:

- [When this article is cited](#)
- [When a correction for this article is posted](#)

[Click here](#) to choose from all of JBC's e-mail alerts

This article cites 63 references, 36 of which can be accessed free at <http://www.jbc.org/content/279/16/16194.full.html#ref-list-1>